From crypts to enteroids: establishment and characterization of avian intestinal organoids

Dan Zhao,[*] Morgan B. Farnell,[*] Michael H. Kogut ,[†] Kenneth J. Genovese,[†] Robert S. Chapkin,[‡] Laurie A. Davidson,[‡] Luc R. Berghman,[*,§] and Yuhua Z. Farnell[*,1]

[*]*Department of Poultry Science, Texas A&M AgriLife Research, Texas A&M University, College Station, TX 77843;* [†]*Southern Plains Agricultural Research Center, Agricultural Research Service, US Department of Agriculture, College Station, TX 77845;* [‡]*Program in Integrative Nutrition & Complex Diseases, Texas A&M AgriLife Research, Texas A&M University, College Station, TX 77843; and* [§]*Department of Veterinary Pathobiology, Texas A&M University, TX 77843*

ABSTRACT Intestinal organoids (**IO**), known as "mini-guts", derived from intestinal crypts, are self-organizing three-dimensional (**3D**) multicellular ex vivo models that recapitulate intestine epithelial structure and function and have been widely used for studying intestinal physiology, pathophysiology, molecular mechanisms of host-pathogen interactions, and intestinal disease in mammals. However, studies on avian IO are limited and the development of long-term cultures of IO model for poultry research is lacking. Therefore, the objectives of this study were to generate crypt-derived organoids from chicken intestines and to optimize conditions for cell growth and enrichments, passages, and cryopreservation. Crypts were collected from the small intestines of birds at embryonic d-19 and ceca from layer and broiler chickens with ages ranging from d 1 to 20 wk, embedded in a basement membrane matrix, and cultured with organoid growth media (**OGM**) prepared in house. The crypt-derived organoids were successfully grown and propagated to form 3D spheres like structures that were cultured for up to 3 wk. Organoids were formed on d one, budding appeared on d 3, and robust budding was observed on d 7 and beyond. For cryopreservation, dissociated organoids were resuspended in a freezing medium. The characteristics of IO upon extended passages and freeze-thaw cycles were analyzed using reverse transcription (**RT**)-PCR, immunoblotting, and live cell imaging. Immunoblotting and RT-PCR using E-cadherin (the marker for epithelial cells), leucine-rich repeat-containing G protein-coupled receptor 5 (LGR5, the marker for stem cells), chromogranin A (the marker for enteroendocrine cells), lysozyme (the marker for Paneth cells), and mucin (the biomarker for goblet cells) confirmed that IO were composed of heterogeneous cell populations, including epithelial cells, stem cells, enteroendocrine cells, Paneth cells, and goblet cells. Furthermore, OGM supplemented with both valproic acid and CHIR99021, a glycogen synthase kinase 3β inhibitor and a histone deacetylase inhibitor, increased the size of the avian IO ($P < 0.001$). To the best of our knowledge, this is the first comprehensive report for establishing long-term, organoid culture models from small intestines and ceca of layer and broiler chickens. This model will facilitate elucidation of the mechanisms impacting host-pathogen interactions, eventually leading to the discovery of pathogen intervention strategies in poultry.

Key Words: three-dimensional cell culture, organoid, crypt, chicken intestines

2022 Poultry Science 101:101642
https://doi.org/10.1016/j.psj.2021.101642

INTRODUCTION

Functional and heterogeneous intestinal organoids (**IO**), also known as "mini guts" or "enteroids", are self-organized three-dimensional (**3D**) organ-like constructs. Intestinal organoids have been well developed and are used to study gastrointestinal diseases, intestinal physiology, and host-pathogen interaction in human medicine (Forbester et al., 2015; Thorne et al., 2018; Chandra et al., 2019). Intestinal organoids fully recapitulate the physiology of intestinal epithelium, containing

Received April 30, 2021.
Accepted November 17, 2021.

[1]Corresponding author: yfarnell@tamu.edu, yuhua.farnell@agnet.tamu.edu (YZF)

stem cells and differentiated cells (enterocytes, goblet cells, Paneth cells and enteroendocrine cells). Intestinal organoids are established from intestinal crypts containing pluripotent stem cells or adult stem cells (Sato et al., 2009; Sato et al., 2011; Forbester et al., 2015). Cultures are maintained in media containing various growth factors targeting several critical signaling pathways. For example, Wnt signals are required for stem cell proliferation and Paneth cell terminal differentiation (Korinek et al., 1998; Farin et al., 2012). Notch signals serve as the enterocyte-secretory switch (van Es et al., 2005). Epidermal growth factor (**EGF**) promotes the mitosis of stem cells (Wong et al., 2012) and bone morphogenetic protein (**BMP**) supports villus formation (Haramis et al., 2004). Compared to traditional 2-dimensional cell lines, 3D IO grown in organoid growth media (**OGM**) containing these factors preserve natural intestine morphology and cell polarity, thereby recapitulating elements of the in vivo environment to enhance cell-to-cell interactions.

This beneficial IO culture system is widely studied in mammalian systems but not extensively in avian research, although there are numerous gastrointestinal diseases and pathogen infections affecting the quality and quantity of poultry products. Currently, avian intestinal epithelial cells as in vitro model systems are not available for studying the mechanism of host-microbiome interaction and for screening of nutrients to improve overall gut health. The majority of avian studies are based on short-term studies of avian primary enterocyte cultures (Caldwell et al., 1993; Velge et al., 2002; Dimier-Poisson et al., 2004; Rath et al., 2018) or commercial mammalian cell lines as a proxy. In the past 10 yr, only few papers described organoids derived from the small intestine of chick embryos (Pierzchalska et al., 2012, 2017, 2019; Panek et al., 2018). These studies demonstrated that prostaglandin E_2 played an important role for the growth of small IO in 18-day-old chicken embryos. Probiotic bacteria and synthetic Toll-like receptor 2 (**TLR2**) ligands also positively influenced IO derived from the small intestine of 19-day-old chicken embryos (Pierzchalska et al., 2017). The migration and fusion of IO originated from the small intestine of 19-day-old chicken embryos were described (Pierzchalska et al., 2019). Li et al. (2018) established organoids from the jejunum of 2- to 3-wk-old layer chickens and demonstrated the villus structure using transmission electron microscopy. However, the establishment of organoids from avian ceca has not been studied extensively. Powell and Behnke (2017) collected chicken ceca from processing plants and established a culture of chicken cecum organoids. However, they did not fully characterize cellular and molecular components of cecum-derived organoids.

In order to support the development of an organoid culture system, new functional growth factors can be selected to optimize organoid growth. Valproic acid (**VA**) plays an essential role in Notch activation as a histone deacetylase inhibitor (Stockhausen et al., 2005; Greenblatt et al., 2007). CHIR99021 (**CHIR**), an activator of the Wnt signaling pathway, can inhibit GSK3β-mediated β-catenin degradation as a specific GSK3 inhibitor (Bain et al., 2007). Valproic acid and CHIR have been shown to increase stem cell proliferation in mice and human IO cultures (Ye et al., 2012; Wang et al., 2016; Langlands et al., 2018). However, no studies to date have examined the effects of VA and CHIR on avian IO development and growth.

Therefore, we cultured crypt-derived IO in a laminin-rich Matrigel and organoid growth media (**OGM**) and assessed IO morphology and cell composition via western blotting, reverse transcription polymerase chain reaction (**RT-PCR**) and immunofluorescence. The effects of small molecules (CHIR and VA) on the growth and development of organoids were examined.

MATERIALS AND METHODS

Experimental Birds

Layer chickens at embryonic d 19 (n = 20) and layer and broiler chickens with ages ranging from d 1 to 20 wk (n = 15) were used. The animal use protocol was approved by Institutional Animal Care and Use Committee of Texas A&M University (IACUC.2016-0270 and 2019-0171).

The Collection of Conditioned Media from L-WRN Cell Cultures

L-WRN cells (ATCC, #CRL-3276), producing Wnt-3A, R-spondin, and noggin factors, were cultured in high glucose DMEM (Gibco, Grand Island, NY) supplemented with 1X penicillin/streptomycin (Gibco) and 10% fetal bovine serum (FBS; HyClone, Logan, UT). The L-WRN CM was collected following the large-scale L-WRN CM production protocol described by Miyoshi and Stappenbeck (2013) and stored at -80°C.

Crypt Isolation

Isolation of crypts followed the protocol previously described by Fujii et al. (2015) with some modifications. Briefly, the intestinal tissues (including duodenum, jejunum, ileum, and ceca) were collected from birds, opened longitudinally and washed 3 times with cold PBS to remove luminal contents. The cleaned intestinal tissues were then cut into 2 to 4 cm pieces and incubated with 2.5 mM EDTA in PBS for 30 min on a shaker with a speed of 300 rpm at 4°C to release crypts. Supernatant fractions enriched in crypts were collected, filtered through a 100-μm and 70-μm cell strainer, and centrifuged at 300 × g for 5 min at 4°C to collect the crypts. Crypt pellets were washed in cold PBS at 300 × g for 5 min, 150 × g for 5 min, and 70 × g for 5 min to remove small debris and single cells.

Intestinal Crypt Culture and the Generation of Organoids

Approximately 500 crypts were suspended in 30 μL of growth factor reduced phenol-free Matrigel (BD Biosciences, San Jose, CA), as shown in Figure 1A. The Matrigel/crypt mix was placed in the center well of a 24-well plate. After 10 min of polymerization, 500 μL of OGM was added to the wells and was changed every other day. The OGM contains Advanced DMEM/F12 (Gibco, Grand Island, NY) supplemented with 1X antibiotic-antimycotic (Gibco), 10 mM HEPES (Sigma, St. Louis, MO), 1X Glutamax (Gibco), 1 mM N-Acetyl-L-Cysteine (ACROS, Pittsburgh, PA), 50 ng/mL EGF (Gibco), 500 nM A83-01 (AdooQ, Irvine, CA), 10 μM SB202190 (AdooQ), 10 μM Y-27632 (AdooQ), 0.02 μM PGE2, and 50% L-WRN cell-derived conditioned media (CM). Live images of the avian IO were captured using an all-in-one BZ-X800 Keyence Fluorescence Microscope (Osaka; Osaka Prefecture, Japan).

Organoid Passaging and Cryopreservation of Organoids

Organoids were split every 4 to 5 d in a 1:4 ratio using TrypLE Express (Gibco) with 10 mM Y-27632 (AdooQ) and plated in 24 well plates.

Organoids were suspended in OGM by pipetting up and down gently and transferred to a 1.5 mL tube. The suspension was centrifuged at 200 $\times$ g for 5 min at room temperature. Organoids were resuspended in 500 μL of freezing medium (OGM: FBS: DMSO = 8:1:1) and kept at -80°C. Frozen organoids were transferred and stored in a liquid nitrogen tank.

Histochemistry

Cecum sections before and after EDTA chelation were fixed in 4% paraformaldehyde for 48 h, washed with PBS twice, dehydrated in 70% ethanol, and embedded in paraffin. The paraffin blocks were cut into 5-μm sections. The sections were deparaffinized and stained with hematoxylin and eosin (H&E).

Avian IO were rinsed 3 times in ice-cold PBS, fixed with 4% paraformaldehyde for 30 min at room temperature in the wells, and rinsed with ice-cold PBS. Fixed organoids in Matrigel were embedded in paraffin and cut into 5-μm sections. The sections were deparaffinized and stained with hematoxylin and eosin.

Immunofluorescence

The sections of avian IO were washed with Tris-buffered saline (**TBS**) containing 0.1% Tween 20 (**TBST**) and blocked using 10% normal goat serum (Vector Laboratories) in TBST for one h at room temperature, incubated with mouse anti E-cadherin (1:250, ab76055, Abcam, Waltham, MA) overnight at 4°C. After 3

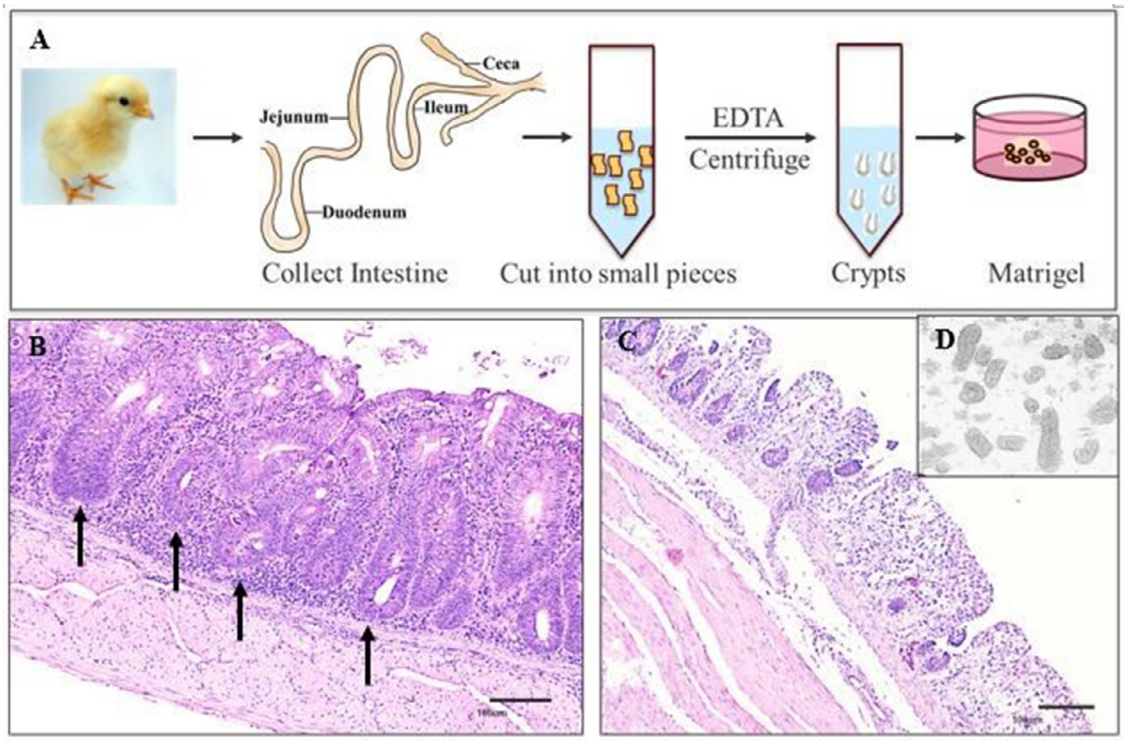

Figure 1. Description of the establishment of crypt-derived 3D avian intestinal organoids. (A) Schematic diagram showing avian intestinal crypts isolated from a broiler chicken. The avian intestines were collected, cut open longitudinally, washed 3 times in cold PBS, cut into small pieces, and incubated in EDTA to release the crypts. The crypts were purified through differential centrifugation and filtration with 100 μm and 70 μm filters. Purified crypts were embedded in Matrigel surrounded in organoid growth media. (B) Representative ceca-cross section stained with hematoxylin-eosin (H&E). Black arrows indicate examples of crypts. Scale bar = 100 μm. (C) Representative image of ceca cross-section stained with H&E after the removal of most crypts following EDTA chelation. Scale bar = 100 μm. (D) Purified crypts after differential centrifugation and filtration.

washes with TBST, the secondary antibody Alexa Fluor 555 goat antimouse IgG (1:1000, ab150118, Abcam) was added and incubated at room temperature for one h followed by 3 times washed with TBST. The stained slides were mounted with one drop of Prolong Diamond Antifade DAPI (Thermo Fisher Scientific,Waltham, MA; P36966) and overlaid with a cover glass. Images were captured by all-in-one BZ X800 Keyence Fluorescence Microscope.

Protein Extraction and Western Blotting

Radioimmunoprecipitation assay (**RIPA**) buffer (Thermo Fisher Scientific, Waltham, MA) was used to extract protein from avian IO. Protein concentration was quantified by a BCA Protein Assay Kit (Thermo Fisher Scientific, Waltham, MA). Fifty micrograms of protein from each sample were resolved onto 4 to 12% SDS-PAGE gradient gels (Bio-Rad, Hercules, CA). Following electrophoresis, proteins were transferred to polyvinylidene difluoride (**PVDF**) membranes by a semi-dry electroblotting system (Bio-Rad, Hercules, CA) at 50 mA for 2 h. The PVDF membranes were blocked in TBST and 5% nonfat milk overnight at 4°C. Membranes were washed 4 times for 10 min in TBST, and then incubated with primary antibody for 4 h. The following primary antibodies were all from Abcam (Cambridge, MA) and used at the indicated dilutions: rabbit anti-Lgr5 (ab75732; 1:500), mouse anti-E cadherin (ab76055; 1:1,000), rabbit antilysozyme (ab391; 1:1,000), mouse antichromogranin A (1:500; Proudman et al., 2003), mouse anti-GAPDH ab8245; 1:10,000). The membrane was washed 4 times in TBST, followed by incubation with a secondary antibody for 1 h at room temperature. The following secondary antibodies were used: horseradish peroxidase (**HRP**)-conjugated goat antirabbit IgG (ab205718; 1:20,000), HRP-conjugated goat antimouse IgG (ab97040; 1:20,000). Enhanced chemiluminescence (ECL) detection reagents (Amersham Pharmacia Biotech, Piscataway, NJ) were employed. The chemiluminescent signals were captured and analyzed by a ChemiDocTM MP Image System (Bio-Rad, Hercules, CA). Immunoblot images were quantified by Quantity One-4.6.1 software (Bio-Rad).

Total RNA Extraction and Reverse Transcription PCR

The avian IO were collected into a 15 mL low-binding centrifuge tube (STEMFULL, Sbio, Cat MS-90150) containing a total 2 mL of TrypLE Express (Gibco, Grand Island, NY). Tubes were placed in a 37°C water bath for 5 min to dissolve the Matrigel. Pellets of IO were collected by sequential centrifugations at 400 × g for 5 min at 4°C and at 1,000 × g for 5 min at 4°C. Total RNA was extracted from purified avian IO using the mirVana miRNA isolation kit (Ambion, Austin, TX) following the manufacturer's manual. Total RNA concentrations were measured by NanoDrop 1000. One microgram of total RNA was reverse transcribed using SuperScript III First-Strand Synthesis System (Invitrogen) following the manufacturer's protocol. Reverse transcription polymerase chain reaction (RT-PCR) was conducted using Powerup SYBR Green Master Mix according to the manufacturer's instruction. The primer sequences used for qRT-PCR are listed in Table 1. Briefly, Power up SYBR Green Master Mix was combined with 10 μM primers and 10 ng cDNA template and loaded onto a 384-well plate. The cycle condition for RT-PCR was performed at 50°C for 2 min, 95°C for 10 min, following 40 cycles of 95°C for 15 s and 60°C for 1 min. Products of

Table 1. Summary of primers of target genes used for RT-PCR analysis.

Target gene		Primer Sequence (5' to 3')		Amplicons (bp)
Reference				
LGR5	For	CCTTTATCAGCCCAGAAGTGA	338	Li et al., 2018
	Rev	TGGAACAAATGCTACGGATG		
E-cadherin	For	ACTGGTGACATTATTACCGTAGCA	226	Tiwari et al., 2013
	Rev	TAGCCACTATGACATCCACTCTGT		
Lysozyme	For	GACGATGTGAGCTGGCAG	225	Wang et al., 2016
	Rev	GGATGTTGCACAGGTTCC		
Chromogranin A	For	TGAATAAAGGGGACACTAAGG	337	Dr. Berghman
	Rev	AGCTCAGCCAGGGATG		
Muc2	For	CAGCACCAACTTCTCAGTTCC	102	Zhang et al., 2015
	Rev	TCTGCAGCCACACATTCTTT		
Olfm4	For	GACTGGCTCTCTGGATGACC	108	Li et al., 2018
	Rev	AGCGTTGTGGCTATCACTTG		
Alpha-SMA	For	AGGACAGCACTGCCCTTGTTT	136	Tavares et al., 2018
	Rev	CCCATACCAACCATCACACCCT		
Vimentin	For	GAAGCTGCTAACTACCAGGACACT	184	Tiwari et al., 2013
	Rev	TAGGCATGTTAATCCTGCTCTCTT		
GAPDH	For	AGAACATCATCCCAGCGT	182	Shang et al., 2014
	Rev	AGCCTTCACTACCCTCTTG		
Beta-Actin	For	TGCTGTGTTCCCATCTATCG	150	Bai al., 2018
	Rev	TTGGTGACAATACCGTGTTCA		

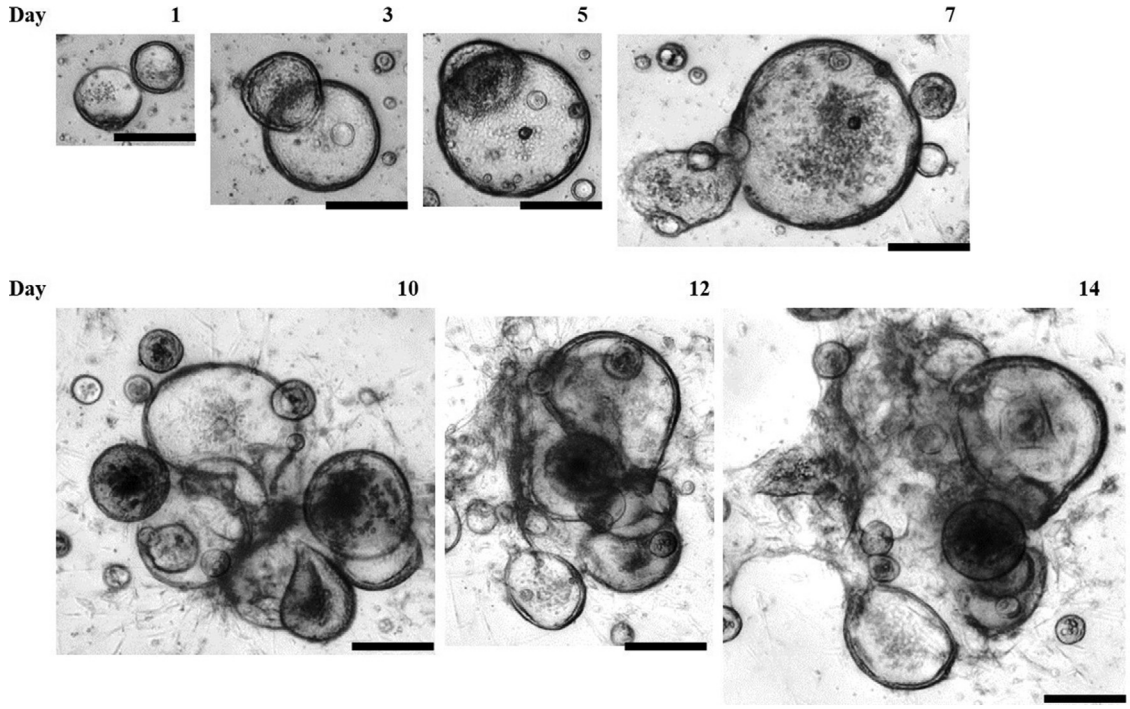

Figure 2. Time course of avian ceca-derived organoid growth from day-one-old broilers. Crypts were collected from the ceca of day-one-old broilers and seeded in Matrigel on a 24-well plate with organoid culture medium. The growth of live organoids was monitored, and images were captured using an all-in-one BZ-X800 Keyence Fluorescence Microscope on the day indicated as numbered. Scale bar = 200 μm.

RT-PCR were separated on a 2% agarose gel in Tris-acetate-EDTA (**TAE**) buffer. To determine the size of the PCR products, a 100 bp DNA ladder was loaded onto the gel. Agarose gel images were captured using a Photo-Doc-It Imaging System (UVP, Upland, CA).

The Effects of OGM Supplemented with VA and CHIR on Avian Small IO Growth

Crypts were isolated from small intestines of 19-day-old chicken embryos (n = 20) and 500 crypts were embedded in Matrigel and cultured in OGM only (Con) and OGM supplemented with 1mM VA (AdooQ), 3 μM CHIR (AdooQ) or a combination of 1 mM VA and 3 μM CHIR for 7 d. Live cultures of the avian IO were imaged with the all-in-one BZ-X800 Keyence Fluorescence Microscope. The size of the avian IO was measured using ImageJ. Experiments were repeated twice at different d, each time with 4 biological replicates for each group.

Statistical Evaluation

The statistical significance of differences in the mean number and size of the avian IO maintained in various conditions was calculated and analyzed by one way ANOVA using JMP14 (SAS Institute Inc., Cary, NC). A P-value ≤ 0.05 was considered statistically significant.

RESULTS

Isolation of Intestinal Crypts of Avian Origin

Crypts were isolated and purified from the small intestines of chicken embryos and the ceca from day-old-broilers and layers. Subsequently, crypts were seeded in Matrigel cultured in OGM as shown in Figure 1A. The presence of crypts in the intestine were stained using H&E and are shown in Figure 1B, highlighted by the black arrows. After EDTA chelation, most of the crypts were released from the intestine (Figure 1C). The released crypts were purified by differential centrifugation and filtration (Figure 1D).

Time Course of Avian Ceca-Derived Organoid Growth

Small intestinal crypts isolated from day-old broilers (N = 4) were seeded in Matrigel on a 24 well-plate with OGM containing growth factors for stem cell proliferation and differentiation. The live culture images of the avian IO were captured from d 1 to 14 (Figure 2). Observation of growth of avian IO in the first 24 h revealed that the majority of the stem cells in the crypts proliferated rapidly to sphere-shaped 3D organoids. The organoids simultaneously transformed into spherical shapes covered with epithelial cells. The organoids continually grew larger during the following 7 d. From d 10 to 14 of culture, the organoids developed branches (Figure 2). The cultured organoids were passaged at least 10 times

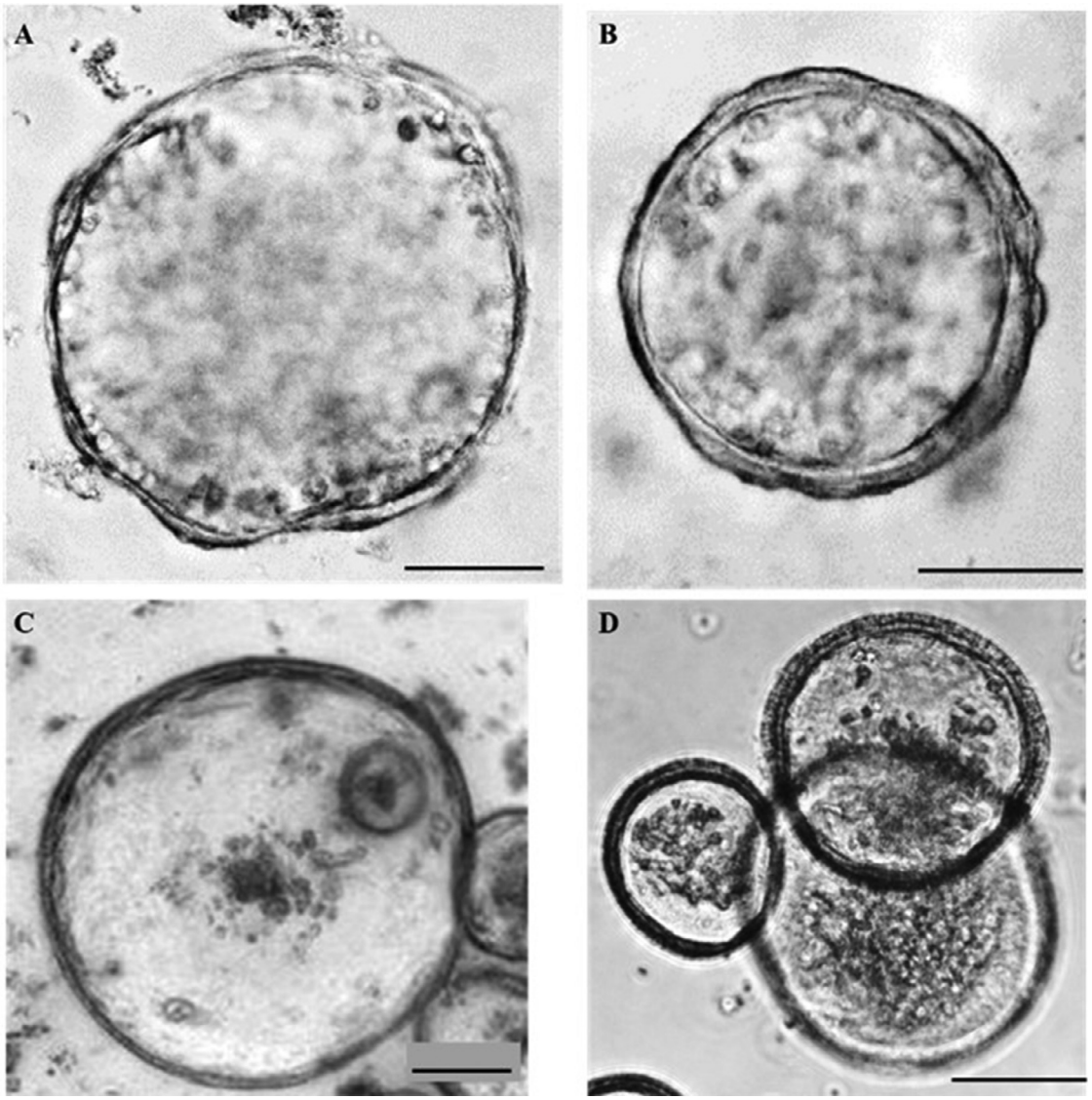

Figure 3. Morphology of avian intestinal organoids.

A representative bright-field image of a cecal organoid derived from 20-wk-old layers (A), a cecal organoid of 4-day-old broilers (B), and small intestines (including duodenum, jejunum, and ileum) of 19-day-old chick embryos (C), and orgnoids derived from ileum of day-14-old broilers after one mo cryopreservation (D) are shown. Image (A) and (B) were captured with an Olympus FV 1000 confocal microscope, image (C) was recorded with an all-in-one BZ-X800 Keyence Fluorescence Microscope, and image (D) was captured with a Nikon Eclipse Ti microscope. All organoids were cultured in the media for 5 d. Scale bar = 100 μm.

(at least the passage time during which we monitored it) and cryopreserved successfully.

Growth Development of Avian Organoids from Ceca and Small Intestines of Broiler, Layer, or Embryo Origins at Different Ages

We also established organoids from the ceca of layer (20-wk-old; Figure 3A) and broiler chickens (4-day-old; Figure 3B) with spherical structures. Representative IO obtained from the small intestine of chicken embryo (embryonic d 19) are shown in Figure 3C, and exhibited the same spherical structure. The growth of orgnoids derived from the ileum of 14-day-old broiler after 30-d cryopreservation was demonstrated in Figure 3D.

Immunofluorescence Staining of Avian Cecal Organoid

Immunofluorescent staining of the cross-section of an organoid highlighted the population of intestinal epithelial cell nuclei (stained with DAPI, Figure 4A) and intestinal epithelial cells using E-cadherin (Figure 4B). Merged image (Figure 4C) showed that these organoids had single cell layers and a closed-loop hollow lumen.

Characterization of Cell Populations of Organoids by Immunoblotting and RT-PCR

To identify cell populations in the cultured avian small IO at d 7 of culture were identified by RT-PCR

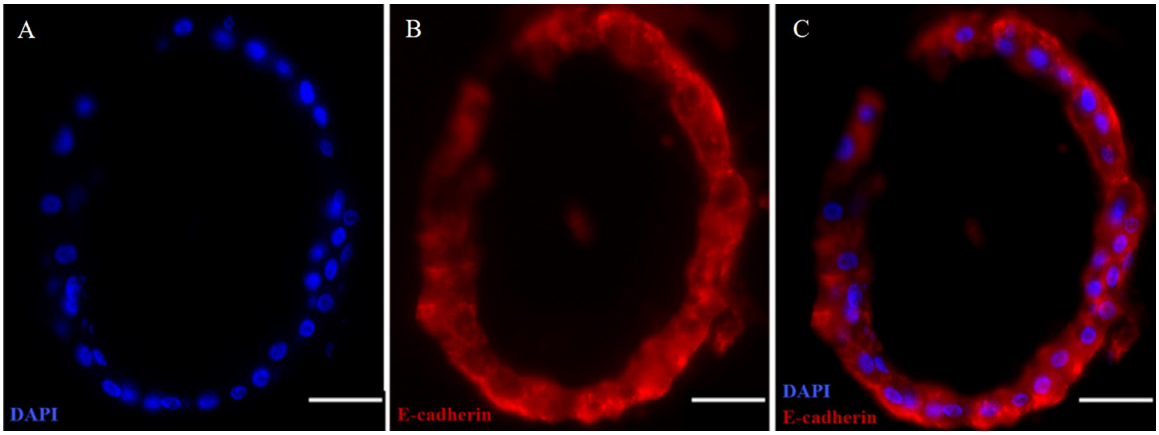

Figure 4. Immunofluorescence staining of avian cecal organoids.

Representative images of immunofluorescence staining of a cecal organoid cross-section using E-cadherin showing a single cell layer, including nuclei of cells stained in blue (DAPI, A). E-cadherin in red (B). Merged image (C). Scale bar = 30 μm. The images were captured by an all-in-one BZ-X800 Keyence Fluorescence Microscope.

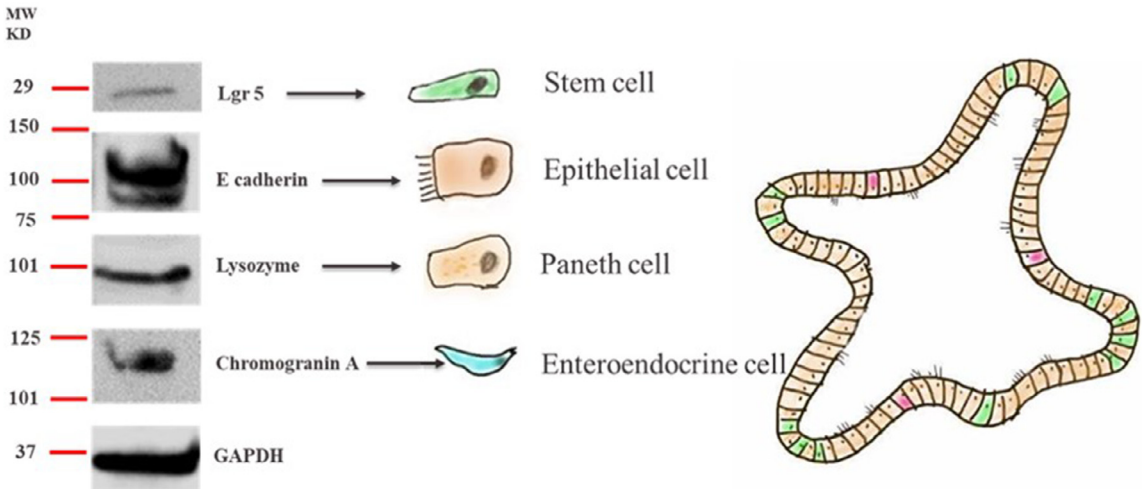

Figure 5. Western blot analysis of different cell types from avian cecal organoids using protein biomarkers.

Cecal organoids in a Matrigel were collected with TrypLE Express and washed with ice-cold PBS. Total protein from organoids was extracted with radioimmunoprecipitation assay buffer (RIPA). Fifty micrograms of protein from cecal organoids were resolved in the 4 to 12% SDS-PAGE gradient gels. Immunoblotting of whole organoid protein extracts showed the presence of Lgr5 (a stem cell marker), E-cadherin (an epithelial cell marker), lysozyme (a Paneth cell marker), and chromogranin A (an enteroendocrine cell marker).

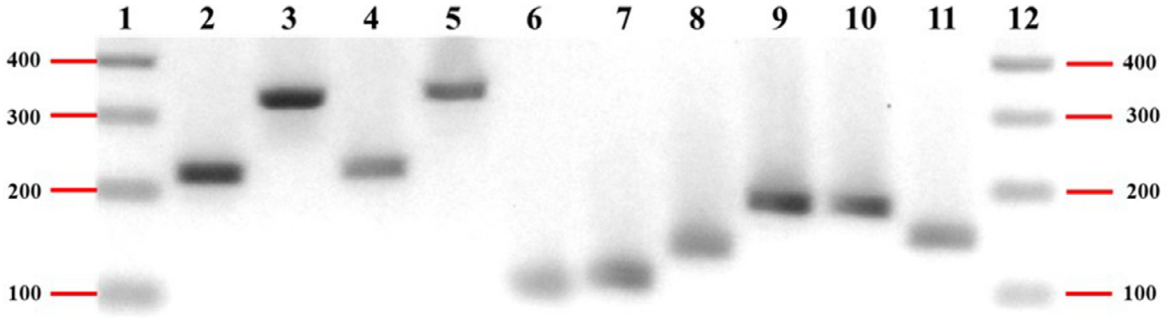

Figure 6. RT-PCR confirms cell populations of organoids using cell marker genes.

Cell populations of avian small intestinal organoids at d 7 of culture were identified by RT-PCR with their biomarker genes. A representative image of RT-PCR results from lane 1 to lane 12 were 100 bp DNA ladder, E-cadherin (epithelial cell marker, 226 bp), Lgr5 (stem cell marker, 338 bp), lysozyme (Paneth cell marker, 225 bp), chromogranin A (enteroendocrine cell marker, 337 bp), Muc2 (goblet cell marker, 102 bp), Olfm4 (stem cell marker, 108 bp), alpha-SMA (myofibroblast marker, 136 bp), vimentin (mesenchymal cell marker, 184 bp), GAPDH (182 bp), actin (150 bp), and 100 bp DNA ladder, respectively.

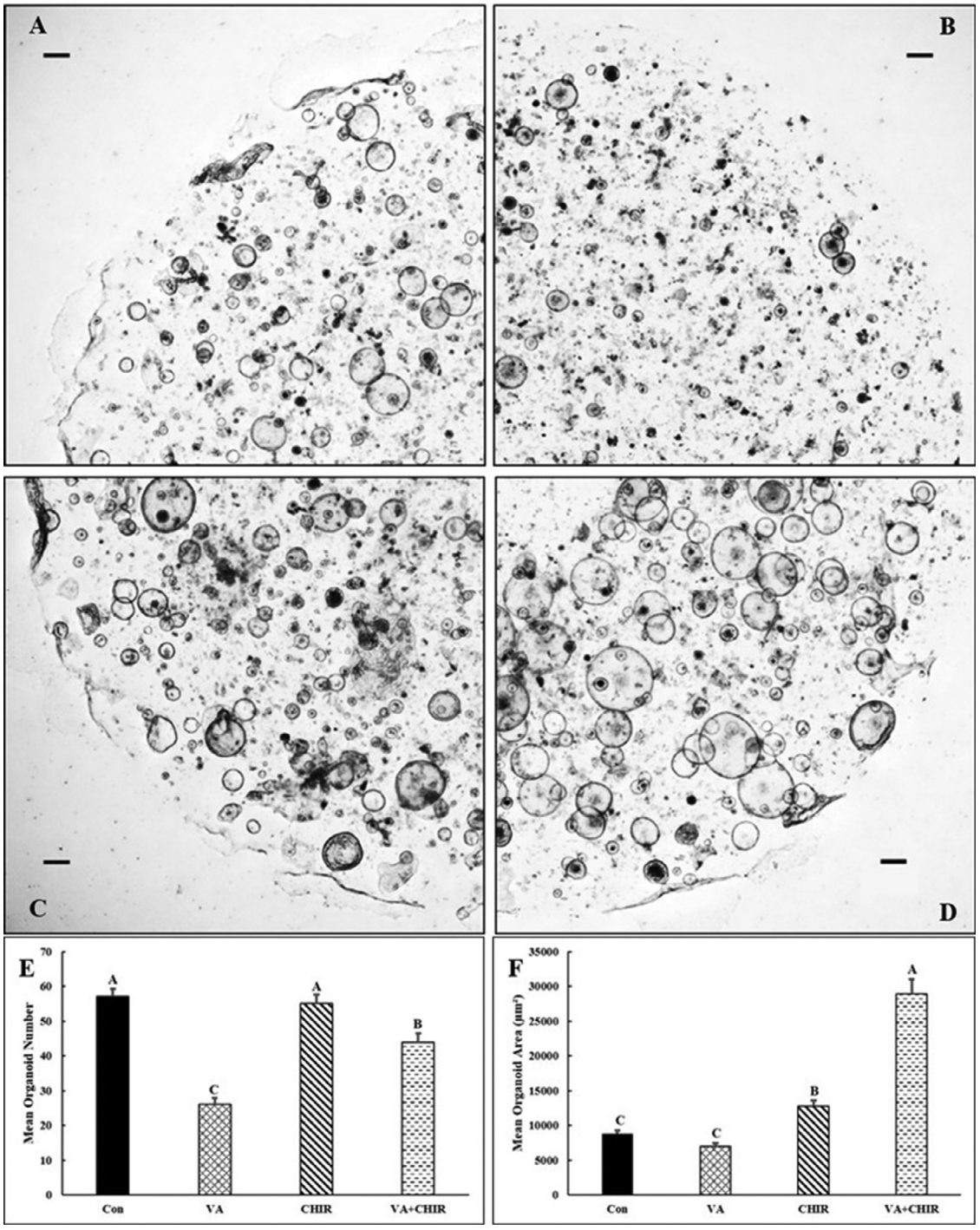

Figure 7. The effect of valproic acid and CHIR99021 on avian small intestinal organoid growth.

Crypts were isolated from small intestines of 19-day-old chicken embryos and embedded in Matrigel and cultured in OGM only (Con) and OGM supplemented with valproic acid (VA), CHIR99021 (CHIR), or a combination of VA and CHIR. Representative images of organoids from 7-d cultures are shown for the Con group (A), VA (B), CHIR (C) and VA+CHIR (D). Scale bars represent 200 μm. Effect of media supplemented with VA and CHIR on the mean organoid numbers (E) and average size of organoids (F) are shown. Experiments were repeated twice on different d, each time with 4 biological replicates for each group. A total of 20 chicken embryos were used. Results are presented as mean ± SEM. The means with a different superscript letter are significantly different from each other ($P < 0.05$).

with their biomarker genes, protein, and total RNA were extracted. Western blotting revealed the presence of lysozyme (a marker for Paneth cells), chromogranin A (a marker for enteroendocrine cells), E-cadherin (a marker for epithelial cells), and Lgr5 (a marker of stem cells; Figure 5). The expression of these genes at the mRNA level was also verified by RT-PCR (Figure 5). Therefore, crypt-derived organoids were populated with epithelial cells that contained stem cells, enteroendocrine and Paneth cells. Furthermore, the RT-PCR results confirmed the expression of Muc2 (a goblet cell marker), Olfm4 (a stem cell marker), alpha-SMA (a myofibroblast marker), and vimentin (a mesenchymal cell marker; Figure 6), confirming the presence of goblet cells, fibroblasts, and mesenchymal cells.

The OGM Supplemented with Both Valproic Acid and CHIR 99021 Increased the Avian IO Size

Valproic acid and CHIR have been used to improve the efficiency of organoid formation in mammalian models. The concentrations of VA and CHIR used in this study have been reported in previous studies examining mammalian species (Yin et al., 2014). To determine how these 2 growth factors influenced avian IO growth, avian IO derived from 19-d embryos were cultured for 7 d in OGM control medium (Con; Figure 7A), OGM supplemented with VA (Figure 7B), CHIR (Figure 7C), or the combined treatment of VA and CHIR (Figure 7D). We found that VA treatment decreased the number of organoids. The numbers of organoids in VA treatment was 45.5% of the Con group (Figures 7B and 7E; $P < 0.0001$). Treatment with CHIR alone did not change the number of organoids (Figure 7E). However, the mean number of organoids in the combined treatment (VA and CHIR) group was 79.7% of the CHIR group ($P = 0.0013$; Figure 7E). In addition, the size of the IO was measured by calculating mean surface area. The mean surface area of the organoids in the VA group was not significantly different compared to the Con group, but the mean surface area of organoids in the CHIR group was 0.4-fold larger ($P = 0.0087$) vs the Con group. The combination of VA and CHIR increased the mean area of organoids by 2.3-fold ($P < 0.0001$) compared to those from the CHIR group.

DISCUSSION

Based on the IO culture protocols for humans and mice (Miyoshi and Stappenbeck, 2013; Fujii et al., 2015; Pierzchalska et al., 2016), we have successfully generated crypt-derived organoids from chicken small intestine and ceca and optimized the conditions for IO growth, passaging, and cryopreservation. The cell populations in crypt-derived IO were characterized, confirming the presences of epithelial cells, stem cells, enteroendocrine, Paneth cells, and goblet cells. Similar to other reports (Pierzchalska et al., 2012, 2017, 2019; Li et al., 2018), we demonstrated the establishment of 3D organoids by growing purified intestinal crypts containing of stem cells and Paneth cells. Compared to single sorted stem cells, isolated crypts are time- and cost-efficient, and easier to handle.

The maintenance of self-renewing stem cells in culture requires 3 major growth factors, Wnt3a, R-spondin, and Noggin (Sato et al., 2009; Clevers, 2016), which can be provided as commercial products (Sato et al., 2009; Pierzchalska et al., 2012; Li et al., 2018), or secreted by the L-WRN (ATCC CRL-3276) cell lines (Miyoshi and Stappenbeck, 2013) that produce all 3 factors. The highly replicable activity of the L-WRN CM was validated over time and between laboratories (VanDussen et al., 2019). The L-WRN CM has been widely used in research to establish mouse and human IO (Miyoshi and Stappenbeck, 2013; Powell and Behnke, 2017; VanDussen et al., 2019). The L-WRN CM supports a cost-effective approach to organoid culture. We are the first group in the poultry field employing L-WRN CM produced by ATCC CRL-3276 cell lines.

The morphology of IO derived from ceca of broiler, layer, and small intestine of chicken embryos all exhibit a spherical shape with a hollow lumen in the center. The morphology of avian IO is similar to the early stage of mouse small intestine IO. Nevertheless, they did not have the regular bud structure that is considered to be the crypt section in the mouse small intestine IO (Yin et al., 2014; Lindeboom et al., 2018).

Avian organoids contained heterogeneous cell populations in our studies. The presence of Lgr5-positive and Olfm4-positive stem cells, Paneth cells, enteroendocrine cells, epithelial cells, and goblet cells were identified by their gene products, detected using western blotting and RT-PCR. Furthermore, our RT-PCR results confirmed the presence of myofibroblast cells (alpha-SMA) and mesenchymal cells (Vimentin). Similarly, Sato et al. (2009) demonstrated the presence of nonepithelial cells in mouse IO derived crypts. We also identified the presence of myofibroblast cells in our organoid culture system, which is consistent with previous reports (Pierzchalska et al. 2017 and 2019). These studies demonstrated that myofibroblasts increased over time more rapidly than the epithelial cells, potentially to promoting IO survival and migration. In vivo, myofibroblasts adjacent to the crypt were reported to regulate the neighboring intestinal stem cells by activating paracrine signals (Williams et al., 1992; Li and Xie, 2005; Crosnier et al., 2006). In addition, coculturing of the intestinal crypts with mesenchymal/stromal cells has been found to promote the intestinal cell growth (Ootani et al., 2009; Lahar et al., 2011; Spence et al., 2011; Li et al., 2016).

The 2 main signaling pathways for the IO culture system are the Wnt and Notch pathways. In this study, we measured the effects of VA and CHIR on the mean number and surface area of the avian IO. We found that VA did not change the size of organoids but decreased the numbers of organoids, and CHIR significantly increased the mean size of organoids without any effect on organoid numbers. It is interesting to note the synergistic effect of CHIR and VA, resulted in the largest mean size of organoids. We speculate that the combined treatment of VA and CHIR increased organoid size by promoting stem cell formation, as demonstrated by Yin et al. (2014). In contrast, supplementation with CHIR induced larger average size of the mice IO, and the combination of CHIR and VA increased the intensity of green fluorescent protein labelled-Lgr5+ stem cells in mice. Ye et al. (2012) described the self-renewing promotion of CHIR in mouse embryo stem cells at the molecular level. Lindeboom et al. (2018) generated stem cell enriched mouse IO following supplementation of CHIR and VA in the organoid culture medium. CHIR alone upregulated mRNA expression of *Olfm4* and *Lgr5* (stem cell biomarker) in organoids from jejunum-derived crypts of

3-wk-old Hyline chickens (Li et al., 2018). In general, larger organoid diameter was associated with stem cells proliferation. The stem cell enriched IO offers a powerful in vitro model to study the mechanism of differentiation of stem cells.

In summary, the avian IO represents a valuable in vitro model for the study of the avian intestinal system and has the potential to replace the use of animals in experiments. Our results show that organoids can be derived from intestines from any age of chicken, consist of multiple cell types and recapitulate the structure and function of the avian intestine. We anticipate the organoid model will play important roles in advancing our knowledge in antimicrobial drug screening, molecular assessment of crosstalk between gut epithelial, immune cells and microbiome, dietary supplement screening to improve gut health in poultry, and vaccine development.

ACKNOWLEDGMENTS

The authors thank the Ag Women Excited to Share Opinions, Mentoring & Experience faculty group in the College of Agriculture and Life Sciences at Texas A&M University for assistance with editing the manuscript. Initial group financial support was through NSF ADVANCE Institutional Transformation Award 1008385, with continued support from the college. Tom Slick Graduate Research Fellowship was provided from College of Agriculture and Life Science at Texas A&M University. This study was supported by USDA NIFA Multistate Hatch # TEX07712 and USDA-ARS (505584-97090). Part of funding was also provided by the Allen Endowed Chair in Nutrition & Chronic Disease Prevention (RSC), and the National Institutes of Health R35-CA197707 (RSC).

DISCLOSURES

All authors declare that they have no known competing financial interests or personal relationships that could have appeared to influence the work reported in this paper.

REFERENCES

Bai, K., C. Feng, L. Jiang, L. Zhang, J. Zhang, L. Zhang, and T. Wang. 2018. Dietary effects of Bacillus subtilis fmbj on growth performance, small intestinal morphology, and its antioxidant capacity of broilers. Poult Sci. 97:2312–2321.

Bain, J., L. Plater, M. Elliott, N. Shpiro, C. J. Hastie, H. Mclauchlan, I. Klevernic, J. S. Arthur, D. R. Alessi, and P. Cohen. 2007. The selectivity of protein kinase inhibitors: a further update. Biochem 408:297–315.

Caldwell, D. J., R. E. Droleskey, M. H. Elissalde, M. H. Kogut, J. R. DeLoach, and B. M. Hargis. 1993. Isolation and primary culture of chicken intestinal epithelial cells retaining normal in vivo-like morphology. J. Tissue Cult. Methods. 15:15–18.

Chandra, L., D. C. Borcherding, D. Kingsbury, T. Atherly, Y. M. Ambrosini, A. Bourgois-Mochel, W. Yuan, M. Kimber, Y. Qi, Q. Wang, and M. Wannemuehler. 2019. Derivation of adult canine intestinal organoids for translational research in gastroenterology. BMC Biol. 17:33.

Clevers, H. 2016. Modeling development and disease with organoids. Cell 165:1586–1597.

Crosnier, C., D. Stamataki, and J. Lewis. 2006. Organizing cell renewal in the intestine: stem cells, signals and combinatorial control. Nat. Rev. Genet. 7:349–359.

Dimier-Poisson, I. H., D. T. Bout, and P. Quéré. 2004. Chicken primary enterocytes: inhibition of Eimeria tenella replication after activation with crude interferon-γ supernatants. Avian Dis. 48:617–624.

Farin, H. F., J. H. Van Es, and H. Clevers. 2012. Redundant sources of Wnt regulate intestinal stem cells and promote formation of Paneth cells. Gastroenterology 143:1518–1529.

Forbester, J. L., D. Goulding, L. Vallier, N. Hannan, C. Hale, D. Pickard, S. Mukhopadhyay, and G. Dougan. 2015. Interaction of *Salmonella* Enterica serovar Typhimurium with intestinal organoids derived from human induced pluripotent stem cells. Infect. Immun. 83:2926–2934.

Fujii, M., M. Matano, K. Nanki, and T. Sato. 2015. Efficient genetic engineering of human intestinal organoids using electroporation. Nat. Protoc. 10:1474.

Greenblatt, D. Y., A. M. Vaccaro, R. Jaskula-Sztul, L. Ning, M. Haymart, M. Kunnimalaiyaan, and H. Chen. 2007. Valproic acid activates notch-1 signaling and regulates the neuroendocrine phenotype in carcinoid cancer cells. Oncologist 12:942–951.

Haramis, A. P., H. Begthel, M. Van Den Born, J. Van Es, S. Jonkheer, G. J. Offerhaus, and H. Clevers. 2004. De novo crypt formation and juvenile polyposis on BMP inhibition in mouse intestine. Science 303:1684–1686.

Korinek, V., N. Barker, P. Moerer, E. van Donselaar, G. Huls, P. J. Peters, and H. Clevers. 1998. Depletion of epithelial stem-cell compartments in the small intestine of mice lacking Tcf-4. Nat. Genet. 19:379–383.

Lahar, N., N. Y. Lei, J. Wang, Z. Jabaji, S. C. Tung, V. Joshi, M. Lewis, M. Stelzner, M. G. Martín, and J. C. Dunn. 2011. Intestinal subepithelial myofibroblasts support in vitro and in vivo growth of human small intestinal epithelium. PLoS One 6:e26898.

Langlands, A. J., T. D. Carroll, Y. Chen, and I. Näthke. 2018. Chir99021 and Valproic acid reduce the proliferative advantage of Apc mutant cells. Cell Death Dis. 9:1–10.

Li, J., J. Li, S. Y. Zhang, R. X. Li, X. Lin, Y. L. Mi, and C. Q. Zhang. 2018. Culture and characterization of chicken small intestinal crypts. Poult. Sci. 97:1536–1543.

Li, L., and T. Xie. 2005. Stem cell niche: structure and function. Annu. Rev. Cell Dev. Biol. 21:605–631.

Li, X., A. Ootani, and C. Kuo. 2016. An air−liquid interface culture system for 3D organoid culture of diverse primary gastrointestinal tissues. Methods Mol. Biol. 1422:33–40.

Lindeboom, R. G., L. van Voorthuijsen, K. C. Oost, M. J. Rodríguez-Colman, M. V. Luna-Velez, C. Furlan, F. Baraille, P. W. Jansen, A. Ribeiro, B. M. Burgering, and H. J. Snippert. 2018. Integrative multi-omics analysis of intestinal organoid differentiation. Mol. Syst. Biol. 14:e8227.

Miyoshi, H., and T. S. Stappenbeck. 2013. In vitro expansion and genetic modification of gastrointestinal stem cells in spheroid culture. Nat. Protoc. 8:2471–2482.

Ootani, A., X. Li, E. Sangiorgi, Q. T. Ho, H. Ueno, S. Toda, H. Sugihara, K. Fujimoto, I. L. Weissman, M. R. Capecchi, and C. J. Kuo. 2009. Sustained in vitro intestinal epithelial culture within a Wnt-dependent stem cell niche. Nat. Med. 15:701.

Panek, M., M. Grabacka, and M. Pierzchalska. 2018. The formation of intestinal organoids in a hanging drop culture. Cytotechnology 70:1085–1095.

Pierzchalska, M., M. Grabacka, M. Michalik, K. Zyla, and P. Pierzchalski. 2012. Prostaglandin E2 supports growth of chicken embryo intestinal organoids in Matrigel matrix. Biotechniques 2:307–315.

Pierzchalska, M., M. Panek, M. Czyrnek, A. Gielicz, B. Mickowska, and M. Grabacka. 2017. Probiotic Lactobacillus acidophilus bacteria or synthetic TLR2 agonist boost the growth of chicken embryo intestinal organoids in cultures comprising epithelial cells and myofibroblasts. Comp. Immunol. Microbiol. Infect. Dis. 53:7–18.

Pierzchalska, M., M. Panek, M. Czyrnek, and M. Grabacka. 2016. The three-dimensional culture of epithelial organoids derived from embryonic chicken intestine. Organoids 1576:135–144.

Pierzchalska, M., M. Panek, and M. Grabacka. 2019. The migration and fusion events related to ROCK activity strongly influence the morphology of chicken embryo intestinal organoids. Protoplasma 256:575–581.

Powell, R. H., and M. S. Behnke. 2017. WRN conditioned media is sufficient for in vitro propagation of intestinal organoids from large farm and small companion animals. Biol. Open. 6:698–705.

Proudman, J. A., S. Clerens, G. Van den Bergh, W. M. Garrett, P. D. Verhaert, F. Vandesande, and L. R. Berghman. 2003. Immunohistochemical localization of chromogranin A in gonadotrophs and somatotrophs of the turkey and chicken pituitary. Gen. Comp. Endocrinol. 132:293–303.

Rath, N. C., R. Liyanage, A. Gupta, B. Packialakshmi, and J. O. Lay. 2018. A method to culture chicken enterocytes and their characterization. Poult. Sci. 97:4040–4047.

Sato, T., J. H. Van Es, H. J. Snippert, D. E. Stange, R. G. Vries, M. Van Den Born, N. Barker, N. F. Shroyer, M. Van De Wetering, and H. Clevers. 2011. Paneth cells constitute the niche for Lgr5 stem cells in intestinal crypts. Nature 469:415–418.

Sato, T., R. G. Vries, H. J. Snippert, M. Van De Wetering, N. Barker, D. E. Stange, J. H. Van Es, A. Abo, P. Kujala, P. J. Peters, and H. Clevers. 2009. Single Lgr5 stem cells build crypt-villus structures in vitro without a mesenchymal niche. Nature 459:262–265.

Shang, Z., L. Guo, N. Wang, H. Shi, Y. Wang, and H. Li. 2014. Oleate promotes differentiation of chicken primary preadipocytes in vitro. Biosci Rep 34:e00093.

Spence, J. R., C. N. Mayhew, S. A. Rankin, M. F. Kuhar, J. E. Vallance, K. Tolle, E. E. Hoskins, V. V. Kalinichenko, S. I. Wells, A. M. Zorn, and N. F. Shroyer. 2011. Directed differentiation of human pluripotent stem cells into intestinal tissue in vitro. Nature 470:105–109.

Stockhausen, M. T., J. Sjölund, C. Manetopoulos, and H. Axelson. 2005. Effects of the histone deacetylase inhibitor valproic acid on Notch signalling in human neuroblastoma cells. Br. J. Cancer. 92:751–759.

Tavares, A. L. P., J. A. Brown, E. C. Ulrich, K. Dvorak, and R. B. Runyan. 2018. Runx2-I is an Early Regulator of Epithelial-Mesenchymal Cell Transition in the Chick Embryo. Dev Dyn. 247:542–554.

Thorne, C. A., I. W. Chen, L. E. Sanman, M. H. Cobb, L. F. Wu, and S. J. Altschuler. 2018. Enteroid monolayers reveal an autonomous WNT and BMP circuit controlling intestinal epithelial growth and organization. Dev. Cell 44:624–633.

Tiwari, A., J. A. Hadley, G. L. Hendricks 3rd, R. G. Elkin, T. Cooper, and R. Ramachandran. 2013. Characterization of ascites-derived ovarian tumor cells from spontaneously occurring ovarian tumors of the chicken: evidence for E-cadherin upregulation. PLoS One. 8: e57582.

van Es, J. H., M. E. van Gijn, O. Riccio, M. van den Born, M. Vooijs, H. Begthel, M. Cozijnsen, S. Robine, D. J. Winton, F. Radtke, and H. Clevers. 2005. Notch/γ-secretase inhibition turns proliferative cells in intestinal crypts and adenomas into goblet cells. Nature 435:959–963.

VanDussen, K. L., N. M. Sonnek, and T. S. Stappenbeck. 2019. L-WRN conditioned medium for gastrointestinal epithelial stem cell culture shows replicable batch-to-batch activity levels across multiple research teams. Stem Cell Res. 37:101430.

Velge, P., E. Bottreau, P. Quéré, P. Pardon, J. C. Nicolle, M. Morisson, D. Bout, and I. Dimier. 2002. Establishment and characterization of partially differentiated chicken enterocyte cell clones. Eur. J. Cell Biol. 81:203–212.

Wang, S., L. Ye, M. Li, J. Liu, C. Jiang, H. Hong, H. Zhu, and Y. Sun. 2016. GSK-3β inhibitor CHIR-99021 promotes proliferation through upregulating β-catenin in neonatal atrial human cardiomyocytes. J. Cardiovasc. Pharmacol. 68:425–432.

Williams, E. D., A. P. Lowes, D. Williams, and G. T. Williams. 1992. A stem cell niche theory of intestinal crypt maintenance based on a study of somatic mutation in colonic mucosa. Am. J. Pathol. 141:773.

Wong, V. W., D. E. Stange, M. E. Page, S. Buczacki, A. Wabik, S. Itami, M. Van De Wetering, R. Poulsom, N. A. Wright, M. W. Trotter, and F. M. Watt. 2012. Lrig1 controls intestinal stem-cell homeostasis by negative regulation of ErbB signalling. Nat. Cell Biol. 14:401–408.

Ye, S., L. Tan, R. Yang, B. Fang, S. Qu, E. N. Schulze, H. Song, Q. Ying, and P. Li. 2012. Pleiotropy of glycogen synthase kinase-3 inhibition by CHIR99021 promotes self-renewal of embryonic stem cells from refractory mouse strains. PLoS One 7:e35892.

Yin, X., H. F. Farin, J. H. Van Es, H. Clevers, R. Langer, and J. M. Karp. 2014. Niche-independent high-purity cultures of Lgr5+ intestinal stem cells and their progeny. Nat. Methods 11:106.

Zhang, Q., S. D. Eicher, and T. J. Applegate. 2015. Development of intestinal mucin 2, IgA, and polymeric Ig receptor expressions in broiler chickens and Pekin ducks. Poult Sci. 94:172–180.